Chapter 9
Mafic Dykes of Rewa Basin, Central India: Implications on Magma Dispersal and Petrogenesis

Trisha Lala, A.K. Choudhary, S.K. Patil, and D.K. Paul

Introduction

Like most Large Igneous Provinces (LIP), mafic dykes are an integral component of the Deccan Volcanic Province. It has been estimated that more than 2,000,000 km^3 of lava erupted over a continental area of 500,000 km^2 in a short span of 0.5 million years (White and McKenzie, 1989) (Fig. 9.1). In the Deccan Volcanic Province (DVP) mafic dykes are abundant in the Western Ghats and Konkan coastal belt in the west and in the Son-Narmada-Tapi river basins but rare in the eastern part (Karkare and Srivastava, 1990). Recent studies of these dykes by Ray et al. (2007), Sheth et al. (2004), Chandrasekharam et al. (1999), Bhattacharji et al. (1996), have brought out their petrological and geochemical details.

The Narmada-Son lineament in central India is a prominent linear feature across India extending to Madagascar. It is considered to be a continental wrench system (Chakraborty et al., 2003) formed in the Precambrian, or a mid-continental rift system (Beane et al., 1986; Shanker, 1991). Mafic dykes have been considered to be the feeder to the mafic flows in parts of the DVP. Sedimentary basins of Gondwana age formed along the Son-Narmada lineament (Chakraborty et al., op.cit.) as extensional or as strike-slip basins. Mafic dykes occur in these basins along well-defined faults. Rajmahal – Bengal Basin–Sylhet basalts (~115 Ma, Baksi et al.1987; ~118 Ma, Kent et al., 2002) occur towards the eastern end of the lineament in eastern India. There are several mafic and ultramafic dykes in the vicinity of the Rajmahal basalt occurrences in the coal-bearing Raniganj and Jharia Gondwana basins. One such prominent dyke, the Salma dyke, a ferrogabbro, was dated at 64.4 ± 0.3 Ma (Kent

D.K. Paul (✉)
Department of Geology, Presidency College, Kolkata 700073, India
e-mail: dalimpaul@yahoo.co.in

T. Lala
Department of Geology, Presidency College, Kolkata 700073, India

A.K. Choudhary
Indian Institute of Technology, Roorkee 247667, Uttaranchal, India

S.K. Patil
Dr. K.S. Krishnan Geomagnetic Research Laboratory, Allahabad 221505, India

R.K. Srivastava (ed.), *Dyke Swarms: Keys for Geodynamic Interpretation*,
DOI 10.1007/978-3-642-12496-9_9,

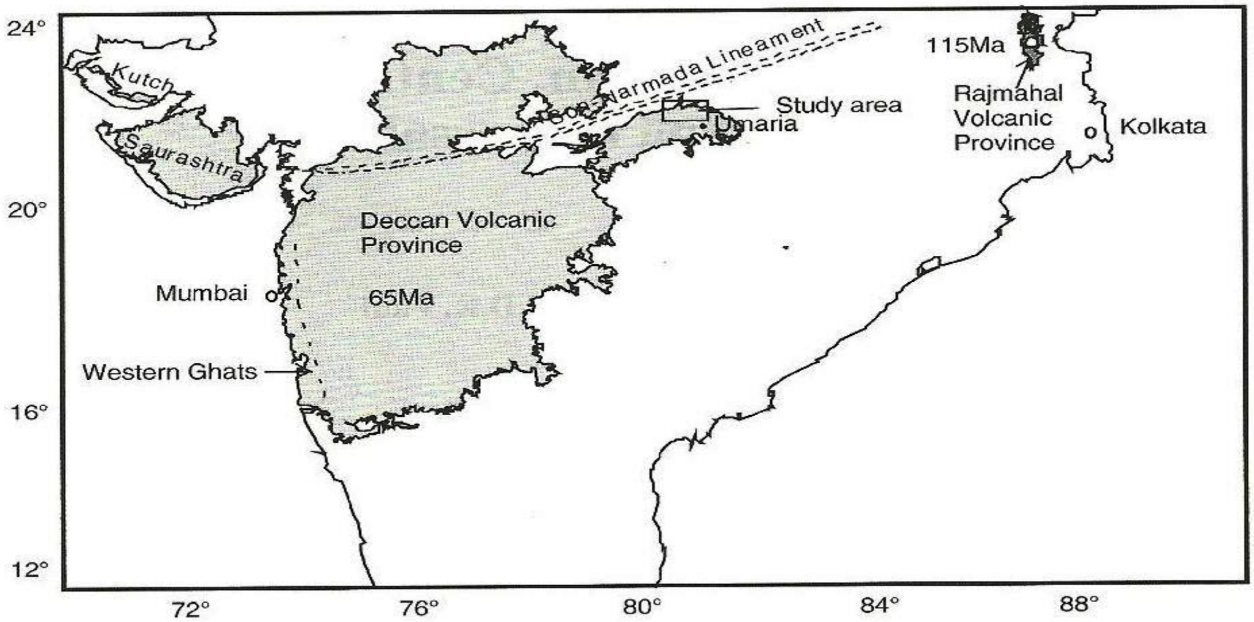

Fig. 9.1 Map showing Deccan Volcanic Province, DVP (65 Ma) and Rajmahal volcanic rocks (115 Ma) in eastern India. The present study area is in the eastern end of DVP

et al., 1997). Though geographically the Salma dyke is closer to the Rajmahal basalt occurrence, the age of 64.4 Ma is very close to that of eruption of Deccan volcanics.

A possibility exists that the magma which was emplaced as the Salma dyke belongs to the Deccan Province but moved eastward at sub-crustal depths. In this scenario similar dykes would be expected in the area between the western Deccan Province and the Rajmahal basalt occurrences.

Detailed study of the mafic dykes of the eastern Deccan Volcanic Province (DVP) is, however, rare in contrast to the dykes of western DVP. We have taken up a petrological and geochemical study of the mafic dykes around Shahdol, Umaria and Chirimiri in central India. These have been collectively discussed as Rewa dykes in this paper. The objective is to explore (1) any petrological linkage between the dykes of the main DVP with those of eastern India, (2) compositional variation between the mafic dykes within the Deccan basalts and the older (Carboniferous) Gondwana basin, and (3) evolutionary changes of magma migration from west to east.

Mode of Occurrence

The Deccan Volcanic Province (DVP) is intruded by a complex dyke-sill network comprising at least three regional scale dyke swarms (Auden, 1949, Deshmukh and Sehgal, 1998; Srivastava et al., 1996; Karkare and Srivastava, 1990; Bondre et al., 2006). The northernmost of these is the ENE-WSW trending Narmada-Satpura-Tapi swarm, which apparently continues westward into the Saurashtra Peninsula. The NNW-SSE trending Konkan or west coast dyke swarm represents the southern arm. The middle arm is much shorter in comparison to other arms and is exposed NE of Mumbai, named the Western Ghats swarm. The area forming the eastern-most fringe area of the Narmada-Satpura-Tapi swarm of mafic dykes that intrude the Gondwana sediments around Shahdol, Manendragarh, Chirimiri and Umaria in the Southern Rewa basin of central India (Fig. 9.2) (Paul et al., 2008) has been studied to assess compositional variation. The orientation and dimensions of twenty-nine dykes have been measured from the published geological maps of the Geological Survey of India (2005). Altogether twelve dykes have been selected for petrological and geochemical studies from an area of about 8,000 km^2. North of Shahdol, one mafic dyke, trending NW-SE is exposed along the Son River (Fig. 9.2) intruding the Gondwana (Permo-Triassic) sediments. It has developed a chilled margin characterized by fine grain size along the contact zone. The exposed dyke is 120 m long with a width of 6 m. Smaller NE-SW trending dykes cut across the main NW-SE dyke here and show thin ramifications into the country rock of Gondwana sandstone. Another large dyke trending NE-SW, is exposed along a nala bed in Akhrar, north of Shahdol. The mafic dykes in Manendragarh also intrude the Gondwana sediments and trend NE-SW (Fig. 9.2). These dykes vary from 200 m to 17 km in length and 4–0 m in width. These dykes also trend NE-SW and have a shorter length varying from 500 m to 2.5 km. However, dykes intruding the Gondwana sediments at Chirimiri show a dominant E-W trending pattern.

Age of the Rewa Dykes

The dykes in the area cut across Gondwana sediments in Shahdol and Chirimiri while those around Umaria cut the Deccan volcanics. Kent et al. (1997, 2002) described the mafic dykes from southwest of Rajmahal Volcanic Province (from Kalidaspur, Raniganj; Meghatari, Koderma) and showed that these dykes were of Cretaceous age, close to the age of the Rajmahal basalts (i.e. around 115 Ma). But the prominent Salma dyke, a ferrodolerite, was of Palaeogene age (64.4 Ma) (Kent et al., 1997).

The dykes of Rewa have not been dated isotopically. As the Umaria dykes cut across the Deccan lavas, these are younger than the flows. Palaeomagnetic determinations have been made on the Shahdol and Chirimiri dykes during the present study. The paleomagnetic results on the dykes are given in Table 9.1. Two dykes from Shahdol RB 5 gave normal polarity (348/–7.25) and RB-13 also show normal polarity (338/–21). Amongst the Chirimiri dykes, RB-61, RB-75 show reverse polarity (180/65; 159/38) and RB-64 shows normal polarity (308/–60). Overall mean polarity for these five dykes was obtained by inverting the reverse polarity. Mean ChRm direction for these five dykes has been computed as $D = 339.53°$, $I = -39.18°$, $\alpha_{95} = 27.26°$ and $k = 8.83$. Palaeomagnetic pole at 40.40°N and 286.62°E has been computed by averaging the Virtual Geomagnetic Pole (Fig. 9.3). This is close to the mean Deccan Super Pole (Vandamme et al., 1991). The palaeomagnetic data, therefore, indicates that the dykes of the eastern DVP are Deccan-related.

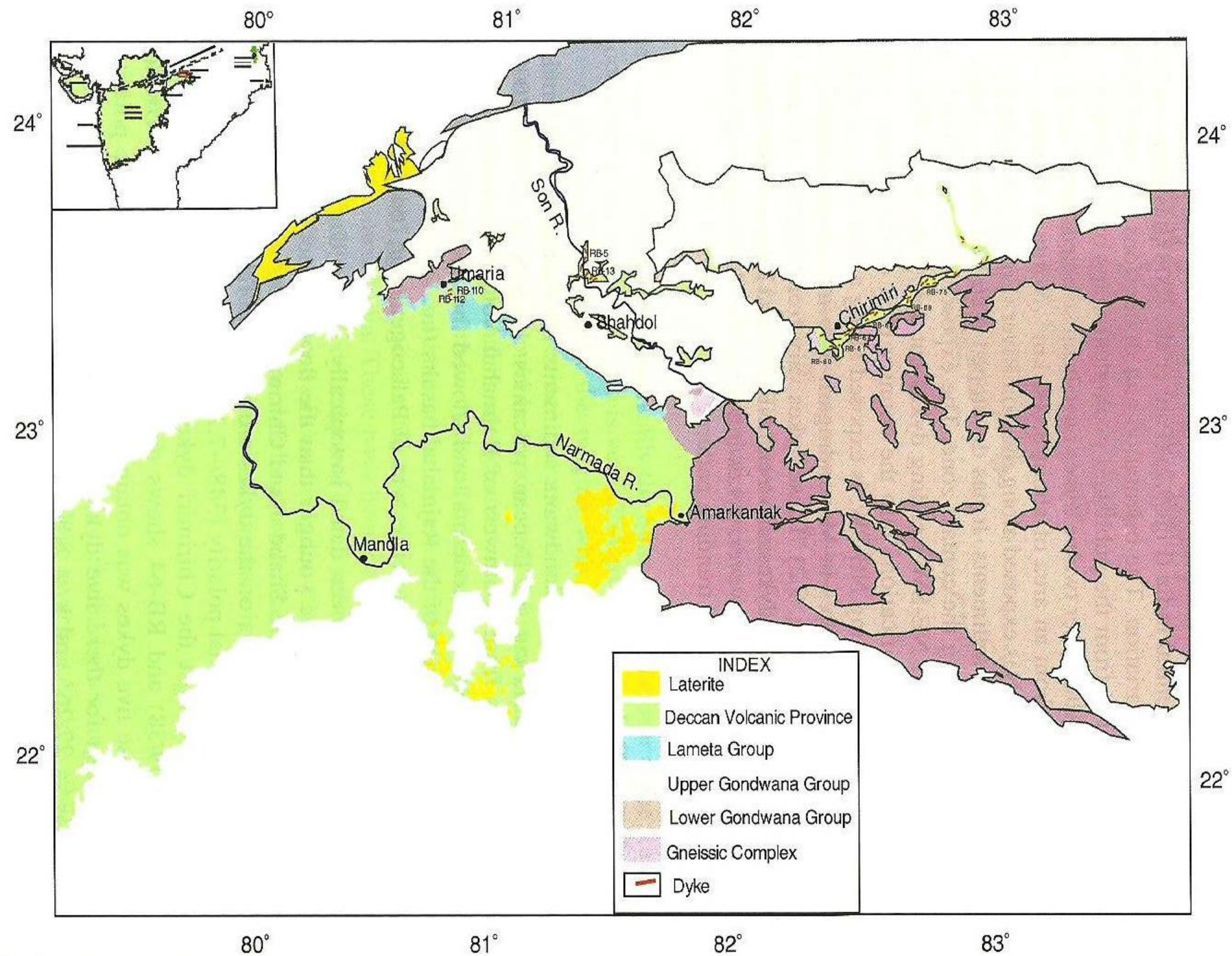

Fig. 9.2 Geological map of the area around Shahdol and Chirimiri based on published Quadrangle Geological maps of Geological Survey of India (2005). The dyke samples are indicated in *bold numbers*, omitting prefix RB, for clarity. The *inset* map shows the extent of Deccan Volcanic Province

Table 9.1 Paleomagnetic results of Rewa dykes

Sample ID	Height	D	I	A_{95}	K	n	VGP Lat	VGP Long	dp	dm	Polarity
RB-5	397	348	−7.25	–	–	1	60.52	286.17	2.53	5.03	N
RB-13	330	338	−21	11.6	33.9	6	49.45	295.59	6.42	12.2	N
RB-61	418	180	65	17	7.46	12	−19.91	82.11	22.14	27.44	R
RB-75	428	159	38	9.6	21.35	12	−41.12	108.4	6.71	11.35	R
RB-64	506	308	−60	6.59	44.35	12	9.82	299.34	7.53	9.96	N

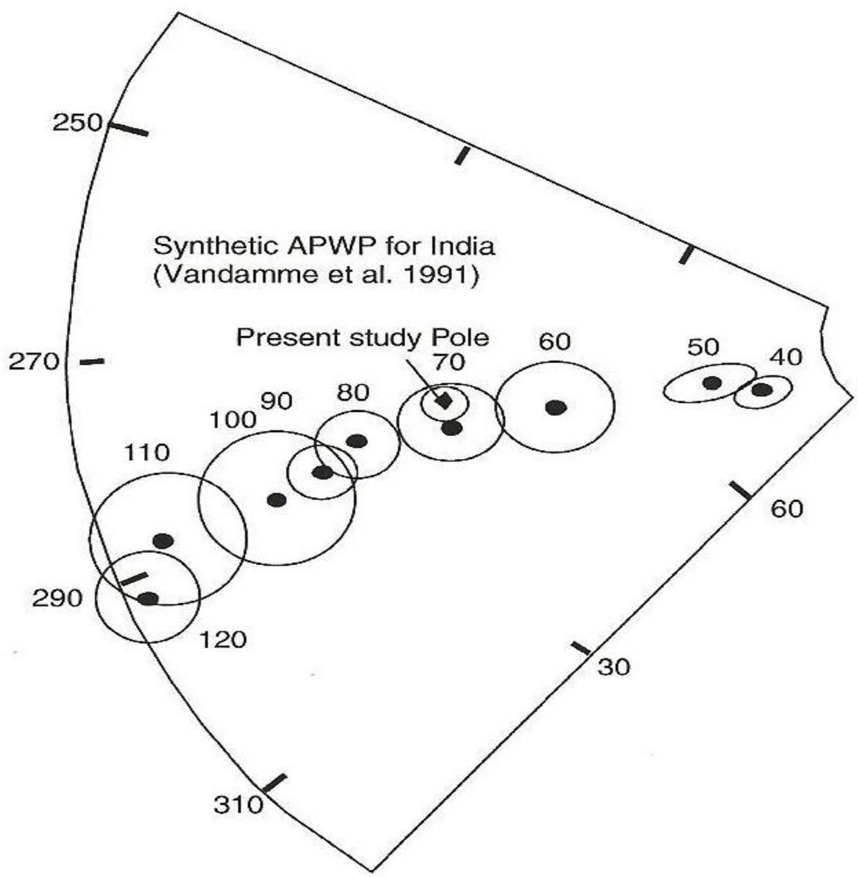

Fig. 9.3 Plot of present study VGP on synthetic APWP for India during the last 120 Ma (APWP from Vandamme et al. 1991)

Petrography

The mafic dykes consist primarily of plagioclase, pyroxene, glass and opaque minerals. Olivine is rare and occurs as anhedral grains (Fo_{29-54}) varying from ~2 to 0.5 mm in size. Phenocrysts of plagioclase feldspar and clinopyroxene sometimes occur in clusters forming glomeroporphyritic texture. Plagioclase also occurs as finer laths forming aggregates. The modal compositions of some of the dyke samples are given in Table 9.2. Phenocryst components (constituting about 39–59 volume %)

Table 9.2 Modal composition of dykes, Rewa Basin

	RB 5	RB 13B	RB 60	RB 66	RB 110	RB 112	RB-68A	RB-64
Plagioclase (P)	28.4	25.9	28.1	39.7	43	29.6	15.7	28.1
Plagioclase (Gm)	40.1	31	36.2	27.9	24.5	27.5	49.3	38.9
Clinopyroxene (P)	15.3	12.7	15.7	13.5	15.6	13.3	12.9	19.8
Clinopyroxene (Gm)	12.1	12.6	6.7	10.7	9.5	10.9	6.9	6.4
Olivine	–	8.4	8.7	–	–	16.2	10.6	–
Opaque	4.1	9.4	4.6	8.2	7.4	2.5	4.6	6.8

P: Phenocryst and Gm: Groundmass

consist of plagioclase feldspar (15.7–43 volume %), clinopyroxene (12.7–19.8 volume %), olivine (8.4–16.2 volume %) and opaque minerals (2.5–9.4 volume %). Magnetite and ilmenite, disseminated in the groundmass, constitute the opaque minerals. Grains are 4–0.4 mm in size. Groundmass consists of glass, microlites of plagioclase feldspar, clinopyroxene and opaque minerals.

Irregular and scattered sericitisation of plagioclase is observed in most of the samples. In particular, the smaller plagioclase laths are more sericitised. The phenocrysts of plagioclase are less altered and mostly fresh, though may be cloudy. The sericitisation has been localised and is not pervasive. But devitrification of glass is pervasive leading to the formation of cryptocrystalline aggregates.

Loss on ignition values have often been used to assess degree of alteration and geochemical mobility of elements. In particular, loss-on-ignition values have been used to assess the reliability of ^{39}Ar–^{40}Ar ages (Baksi, 1987). However, no definite correlation of loss-on-ignition with ^{39}Ar–^{40}Ar ages has been documented. In the samples of our study, the LOI values vary from 0.94 to 1.24% (Table 9.3). Two samples, RB 110 and RB 64, have higher LOI of 2.21 and 2.79% respectively. These two samples are not petrographically different from the other samples, nor do they differ in trace element abundances (see Table 9.2). Although RB 5 has high Ba, Rb and Th compared to other dykes, the LOI value is low.

Mineral Composition

Major element compositions of minerals of the dykes were determined by wavelength dispersive method with a CAMECA SX100 electron microprobe using natural mineral and synthetic standards. Accelerating voltage of 20 kV and beam current of 20 nA was used.

Compositions of representative minerals of four dykes are given in Table 9.4. Sample RB 13a is from the core and RB 13d is from the border zone (Fig. 9.2) of the Son River dyke. The composition of the plagioclase in RB 13a varies from An_{42} to An_{79}. In a zoned plagioclase phenocryst, 250 μm long, the core has composition $An_{71.6}$ to $_{79.9}$, but the rim has composition of An_{42} to An_{59} indicating a prolonged crystallisation. In contrast, in the medium sized 250 μm long plagioclase in RB 13d the composition varies from $An_{62.5}$ to $An_{64.8}$. The anorthite content in the finer

Table 9.3 Major oxide (wt%), trace elements (ppm) and normative composition of Rewa dykes

Sample I.D	RB-64	RB-60	RB304	RB-68a	RB-66	RB112	RB110	RB-75	RB61	RB-5	RB13b	RB13d	Avg	JB-2	JB-2 certified value[a]
SiO_2	49.2	48.6	50.9	48.4	50.5	49.1	49.4	47.3	49.6	49.2	48.2	48.3	49.1	53.21	53.2
TiO_2	2.79	2.89	3.10	3.01	3.23	3.80	3.05	2.58	2.50	2.78	1.93	1.85	2.79	1.19	1.19
Al_2O_3	14.8	13.0	14.4	12.2	14.0	12.4	14.0	12.6	14.8	15.1	15.2	15.9	14.03	14.65	14.67
Fe_2O_3	14.3	14.8	14.3	15.9	14.9	16.1	14.8	16.4	14.3	14.0	13.4	13.0	14.66	14.32	14.34
MnO	0.17	0.18	0.17	0.19	0.17	0.2	0.17	0.2	0.17	0.16	0.16	0.16	0.18	0.19	0.2
MgO	5.40	7.20	4.23	7.32	4.43	4.65	4.96	8.57	5.28	5.35	6.97	7.05	5.95	4.61	4.66
CaO	9.86	10.5	7.95	10.1	9.53	9.43	9.63	10.1	9.19	8.13	9.19	9.23	9.40	9.86	9.89
Na_2O	2.93	2.41	1.97	2.19	2.53	2.52	2.15	2.30	1.85	2.75	2.72	2.69	2.42	2.01	2.03
K_2O	0.69	0.42	0.64	0.57	0.77	0.57	0.65	0.51	0.37	0.82	0.37	0.36	0.56	0.41	0.42
P_2O_5	0.36	0.31	0.35	0.34	0.47	0.39	0.37	0.32	0.25	0.34	0.20	0.20	0.33	0.09	0.1
LOI	2.79	0.97	0.94	1.24	1.15	0.94	2.21	1.05	1.01	1.25	1.24	1.10			
Total	**103.29**	**101.28**	**98.95**	**101.46**	**101.68**	**100.1**	**101.39**	**101.93**	**99.32**	**99.88**	**99.58**	**99.84**	**99.37**	**100.54**	**100.7**
Norm															
Q	0.42	0.58	11.14	1.25	5.8	5.07	5.83	0.001	7.68	2.67	0.0006	2.14	–	–	–
Or	4.08	2.47	3.78	3.36	4.55	3.36	3.84	3.01	2.18	4.84	2.18	2.12	–	–	–
Plag	49.9	43.74	45.16	40.24	45.9	42.1	44.75	41.95	46.57	49.62	51.11	52.94	–	–	–
Di	17.65	21.69	7.17	21.5	16.34	20.92	15.52	20.65	10.75	10.17	13.23	11.67	–	–	–
Hy	16.95	20.04	18.72	21.47	15.22	13.95	16.97	15.66	20.22	20.17	20.38	24.1	–	–	–
Ol	–	–	–	–	–	–	–	7.77	–	–	2.3	–	–	–	–
Mt	4.08	4.24	4.08	4.55	4.27	4.6	4.21	4.69	4.08	4.00	3.82	3.72	–	–	–
Il	5.32	5.51	5.89	5.7	6.08	7.22	5.89	4.97	4.75	5.32	3.61	3.61	–	–	–
Ap	0.78	0.67	0.76	0.74	1.02	0.84	0.8	0.69	0.54	0.71	0.43	0.43	–	–	–

Table 9.3 (continued)

Sample I.D	RB-64	RB-60	RB304	RB-68a	RB-66	RB112	RB110	RB-75	RB61	RB-5	RB13b	RB13d	Avg	JB-2	JB-2 certified value[a]
Trace elements ppm															
Sc	33.3	31.0	28.9	37.9	31.9	39.4	39.0	33.5	29.9	35.3	38.0	39.8	34.8	55.373	54.4
V	383	314	376	395	328	497	498	412	363	427	404	410	400.7	568.483	578
Cr	47.9	54.4	35.8	58.8	29.1	31.7	30.8	47.6	42.3	42.9	57.3	62.1	45.1	27.783	27.4
Co	65.6	61.3	46.3	69.3	63.0	63.9	56.9	66.8	53.7	74.4	79.2	80.1	65.0	39.587	39.8
Ni	13.9	54.0	16.1	19.3	12.3	25.4	25.8	17.4	27.9	23.2	34.7	36.5	25.6	14.197	14.2
Cu	277	223	278	272	356	327	353	252	238	300	211	216	275	229.381	227
Zn	156	116	88	193	159	97	134	152	73	150	119	122	130	110.299	110
Ga	21.5	19.0	22.6	20.6	25.1	26.6	27.3	22.6	21.5	25.6	22.1	22.3	23.1	17.068	17
Rb	15.2	6.4	18.7	12.9	15.4	10.4	15.5	7.71	7.88	25.5	9.83	9.87	13.0	6.192	6.2
Hf	1.34	1.18	4.88	1.35	1.94	5.34	5.16	1.23	3.25	5.41	3.37	3.44	3.16	1.449	1.42
Pb	3.23	3.45	4.575	3.20	4.35	5.07	6.43	3.06	3.451	4.79	4.66	4.52	4.23	5.432	5.4
Sr	277	195	194	186	246	226	238	235	209	210	223	224	222	178.581	178
Y	36.4	35.0	40.9	36.9	49.7	45.9	44.7	34.6	30.8	47.0	31.6	32.3	38.8	25.007	24
Zr	44.5	38.5	214.4	43.6	64.5	232.8	222.8	39.7	145.7	247.8	149.1	150.8	132.8	51.952	51.4
Nb	9.35	7.09	16.9	8.81	12.4	18.4	16.1	7.18	12.3	20.8	12.2	12.38	12.82	0.774	0.8
Cs	2.05	0.90	0.55	0.44	0.78	0.13	0.19	1.07	0.83	1.55	0.32	0.28	0.76	0.911	0.9
Ba	148	73.5	127	153	173	133	177	74.6	94.5	292	83.8	77.3	134	207.082	208
Th	–	0.86	2.85	1.03	1.57	1.37	1.45	0.76	1.204	3.01	1.41	1.49	1.55	0.333	0.33

[a]JB-2 Reference: Govindraju K (1994).

Table 9.4 Representative mineral composition of Rewa dykes

	Plagioclase					Pyroxene							Olivine		Glass			Magnetite		Illmenite
Sample	RB-13A		RB-13D			RB-13A	RB-13D	RB-5					RB-13D		RB-5			RB-13D	RB-5	RB-5
Position		Rim	Core	Rim	Rim		Core	Rim		Core		Rim	Core	Rim						
Comment					**80 µ**	**80 µ**	**50 µ**													
SiO_2	53.82	57.81	49.89	52.96	51.68	47.83	50.03	51.12	50.31	50.65	51.33	50.68	35.09	31.8	68.38	68.48	72.26	0.05	0.11	0.04
TiO_2	0.06	0.03	0.04	0.03	0.07	2.02	1.03	1.1	1.23	1.15	0.96	1.3	0	0.14	0.04	0.05	0.02	25.26	23.3	50.72
Al_2O_3	27.69	25.61	30.62	28.4	28.66	4.15	2	1.78	1.81	1.91	1.71	1.94	0	0.01	14.12	15.46	15.7	1.74	0.86	2.06
CaO	12.01	8.95	14.95	12.49	13.46	18.53	13.94	14.69	14.49	14.25	11.22	18.13	0.37	0.44	1.07	0.07	1.46	0	0.42	0.12
Cr_2O_3	0	0	0.04	0	0.05	0.02	0.01	0.14	0.01	0.08	0	0.25	0	0	0.01	0	0	0.04	0.02	0.00
FeO	0.91	0.71	0.5	0.37	0.69	12.25	16.8	18.09	17.41	13.62	17.11	14.21	37.72	53.7	0.39	0.15	0.33	68.54	67.42	47.56
MnO	0	0	0	0.02	0	0.19	0.4	0.32	0.29	0.37	0.38	0.28	0.42	0.81	0.03	0.03	0	0.47	1.41	0.35
MgO	0.43	0.03	0.17	0.14	0.15	13.15	14.47	12.99	13.68	15.22	16.43	12.78	25.31	12.04	0.07	0.01	0.04	0.35	0.04	0.30
Na_2O	4.51	6.3	3.19	4.52	3.84	0.2	0.23	0.21	0.17	0.21	0.07	0.24	0.02	0	1.34	1.01	4.57	0.01	0	0.00
K_2O	0.2	0.36	0.08	0.12	0.15	0	0.02	0.02	0.02	0	0	0.05	0	0.03	11.55	13.27	4.57	0.01	0	0.00
BaO	0	0	0	0	0	0.08	0.02	0.02	0	0	0	0	0	0	0	0.06	0.43	0.4	0.4	0.80
P_2O_5	0	0.02	0.02	0	0	0.09	0.04	0.03	0.04	0	0.02	0.1	0.04	0.11	1.15	0	0.01	0.02	0	0.00
Total	**99.624**	**99.83**	**99.51**	**99.05**	**98.75**	**98.51**	**98.98**	**100.5**	**99.47**	**97.48**	**99.23**	**99.96**	**98.97**	**99.07**	**98.15**	**98.59**	**99.39**	**96.88**	**93.98**	**101.95**
Oxygens	8	8	8	8		6	6	6	6	6	6	6	4	4				4	4	6
Si	2.436	2.595	2.286	2.418	2.377	1.801	1.881	1.903	1.888	1.904	1.906	1.887	0.997	0.991	3.026	2.998	3.039	0.002	0.003	0.00
Ti	0.002	0.001	0.001	0.001	0.002	0.057	0.029	0.031	0.035	0.033	0.027	0.036	0	0.003	0.001	0.002	0.001	0.676	0.457	0.63
Al	1.477	1.355	1.654	1.528	1.554	0.184	0.089	0.078	0.08	0.085	0.075	0.085	0	0	0.737	0.798	0.778	0.073	0.026	0.04
Cr	0	0	0.001	0	0.002	0.001	0	0.004	0	0.002	0	0.007	0	0	0	0	0	0.001	0	0.00
Fe3	0.039	0.021	0.021	0.021	0.021	0.082	0.082	0.081	0.082	0.082	0.081	0.081	0.009	0.01	0.256	0.253	0.243	0.305	1.054	0.67
Fe2	0.034	0.027	0.019	0.014	0.027	0.386	0.528	0.563	0.547	0.428	0.531	0.442	0.897	1.4	0.014	0.005	0.012	2.041	0.415	0.66
Mn	0	0	0	0.001	0	0.006	0.013	0.01	0.009	0.012	0.012	0.009	0.01	0.021	0.001	0.001	0	0.014	0.031	0.01
Mg	0.029	0.002	0.012	0.01	0.01	0.738	0.811	0.721	0.765	0.853	0.909	0.709	1.072	0.559	0.005	0.001	0.003	0.019	0.002	0.01
Ca	0.582	0.431	0.734	0.611	0.663	0.747	0.562	0.586	0.583	0.574	0.446	0.723	0.011	0.015	0.051	0.003	0.066	0	0.012	0.00
Na	0.396	0.548	0.283	0.4	0.342	0.015	0.017	0.015	0.012	0.015	0.005	0.017	0.001	0	0.115	0.086	0.373	0.001	0	0.00
K	0.012	0.021	0.005	0.007	0.009	0	0.001	0.001	0.001	0	0	0.002	0	0.001	0.653	0.742	0.245	0	0	0.00
Sum	**5.008**	**5**	**5.018**	**5.01**	**5.008**	**4.016**	**4.013**	**3.993**	**4.002**	**3.987**	**3.992**	**4**	**2.998**	**3.001**	**4.86**	**4.889**	**4.759**	**3.133**	**2**	**2.01**

grains in the groundmass is comparable. One plagioclase grain enclosed entirely within a clinopyroxene has anorthite content of $An_{64.1}$. In another dyke sample RB 68a (Table 9.4) the plagioclase shows a wide variation of anorthite content ($An_{42.3}$ to $An_{66.5}$). This also reflects a prolonged crystallisation history.

The clinopyroxene grains in RB13a have composition ranging from $Wo_{38.3}Fs_{23.9}En_{37.8}$ to $Wo_{34.5}Fs_{41}En_{24.5}$. It is clear that the fine clinopyroxenes have higher Fe with decreasing Mg. In the sample RB13d collected from the border zone, the clinopyroxenes show significant variation in CaO and MgO from core to rim ($Wo_{38.8}Fs_{19.1}En_{42.1}$ to $Wo_{26.9}Fs_{57.1}En_{16}$). The clinopyroxenes from RB 5 show variation from $Wo_{32.3}Fs_{33.6}En_{32.1}$ to $Wo_{24.8}Fs_{29.2}En_{45.9}$. One large grain, 250 μm long, of clinopyroxene has been analysed from rim to rim. Variation of some constituents across the grain is shown in Table 9.4.

The opaque minerals that occur in the groundmass mostly as anhedral grains include titaniferous magnetite. TiO_2 content varies from 23.9 to 29.7 wt% and total iron as FeO varies from 63.9 to 68.5 wt%. The few ilmenites analysed show rather uniform composition: Fe as FeO around 47% and TiO_2 around 5% (Table 9.4).

Geochemistry

Samples for geochemical analyses were selected on the basis of petrographic freshness. Small chips of fresh rocks were cleaned with water and crushed in a Jaw crusher and Pulveriser. Between crushing and pulverising, an aliquot of the second sample was processed to remove any memory of the first sample. Major and trace element (including rare earth elements) abundances of twelve mafic dykes are presented in Table 9.3. The major element analyses were carried out using X-ray fluorescence technique with a Philips–PRO PW 2,440 fully automatic, microprocessor controlled X-ray spectrometer equipped with a 4 KW X-ray generator. International rock standards of US Geological Survey and Geological Survey of Japan were used to prepare calibration curves. Total iron was measured as Fe_2O_3. The trace elements were determined using a Perkin Elmer SCIEX, Model 6,100 ELAN DRCII ICP-Mass Spectrometer with a Meinhard nebulizer for sample introduction (see Balaram and Gnaneshwar Rao, 2003 for details). The major and trace element analyses were carried out at the National Geophysical Research Institute at Hyderabad. The major and trace element compositions of the International Standard, JB2, were determined during the present analysis. The results on JB2, given in Table 9.3, indicate the accuracy of the present data.

Of the twelve samples analysed, ten are quartz-normative, and the other two are olivine-normative. All the samples plot in the basalt field in a total alkali-silica diagram (Le Bas et al., 1986) and are of sub-alkaline variety (Irvine and Baragar, 1971). Two samples from the Son River bed (Table 9.3) have the lowest TiO_2 contents of 1.85 and 1.93% and P_2O_5 (0.2%). The dyke samples of Sangamner (Bondre et al., 2006) and Pachmari (Sheth et al., 2009) are very close to our samples in the TAS diagram (Fig. 9.4). The concentration of incompatible trace elements is variable (e.g. Zr from 38.5 to 247.8 ppm, Y from 31.6 to 49.7 ppm, Nb from 7 to 20.8 ppm). When P_2O_5 is plotted against Zr, the Chirimiri dykes form a cluster different from

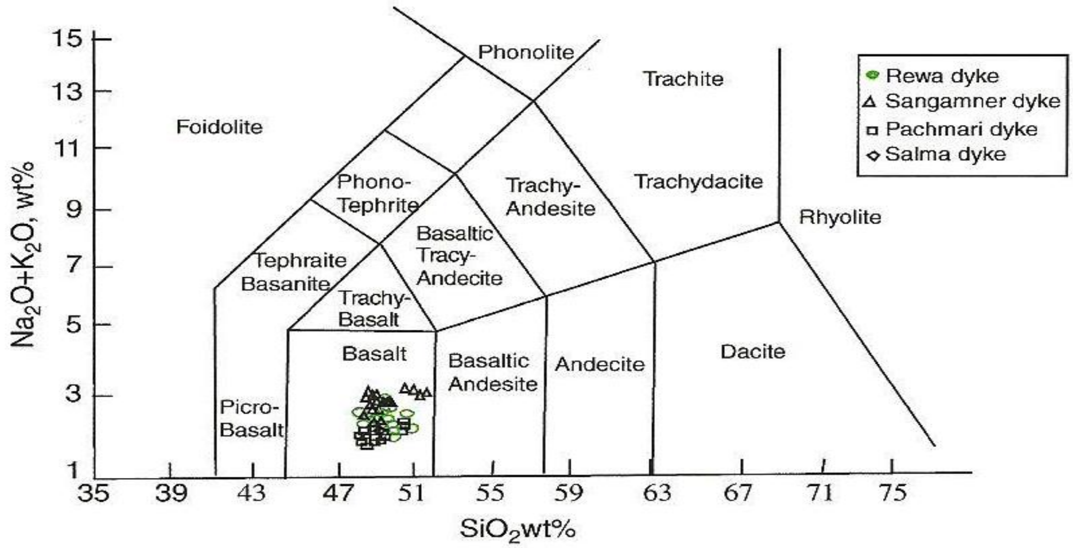

Fig. 9.4 Total alkali-silica diagram (Le Bas et al., 1986) showing Rewa dykes (*present study*), Pachmari dykes (Sheth et al., 2009), Sangamner dykes (Bondre et al., 2006) and Salma dykes from eastern India (Kent et al., 1997). All the dyke samples fall in an overlapping field

the others and follow a different tend (Fig. 9.5a). This clustering is a reflection of lower Zr contents in the Chirimiri dykes (Table 9.3). In a plot of the incompatible trace element ratios, Nb/Zr vs Zr/Y, also the Chirimiri dykes fall in a different group (Fig. 9.5b) separating these from the Shahdol dykes. Significantly, in a P_2O_5 vs TiO_2 plot, the dykes including the Chirimiri samples show a positive correlation (Fig. 9.5c) indicating fractional crystallisation. This is corroborated by the variation of Cr with MgO (Fig. 9.5d) and of Nb/Y against Zr (not shown). Large variations of Zr and TiO_2 contents in Deccan basalts, as found in the dykes of this study, were interpreted to indicate very extensive fractionation (Keays and Lightfoot, 2009). The composition of the Salma dyke from near the Rajmahal volcanic field (Kent et al., 1997) is also similar to the mafic dykes of the Deccan Volcanic Province, although some elements e.g. Zr, Y are similar to the Rajmahal basalts (see Patil and Arora, 2008). Among the samples, the samples RB 13b, RB 13d (Son River) and RB 60, RB 75 (from Chirimiri in the north eastern part) have higher MgO and lower CaO than the others. Also ΣREE contents are comparatively lower in the Son River dykes (86.44 ppm in RB 13b and 87.87 ppm in RB 13d) (Table 9.5). Among all the other Rewa dykes of this study, ΣREE varies from 83.83 to 141.69 ppm.

The REE's show moderate fractionation (Fig. 9.6) with $(La/Yb)_n$ varying from 2.1 to 3.6 on a chondrite-normalised plot, using the chondrite abundances of Evensen et al. (1978). There is a variation in the REE abundances, but the chondrite-normalised plots are very similar. Two samples, RB 61 and RB 75, have lower REE abundances than the others. There is an overlap in the chondrite-normalised fields of the mafic dykes and that of the Deccan flows from the neighbouring areas of Shahdol (Paul et al., 2008). Primitive mantle-normalised (Sun and McDonough, 1989) plots of selected incompatible trace elements (Fig. 9.7) indicate a prominent positive Pb peak between Ce and Sr in all the samples, and a negative Zr-Hf trough, between Nd and Sm. All the elements plotted in Fig. 9.7 show enrichment of

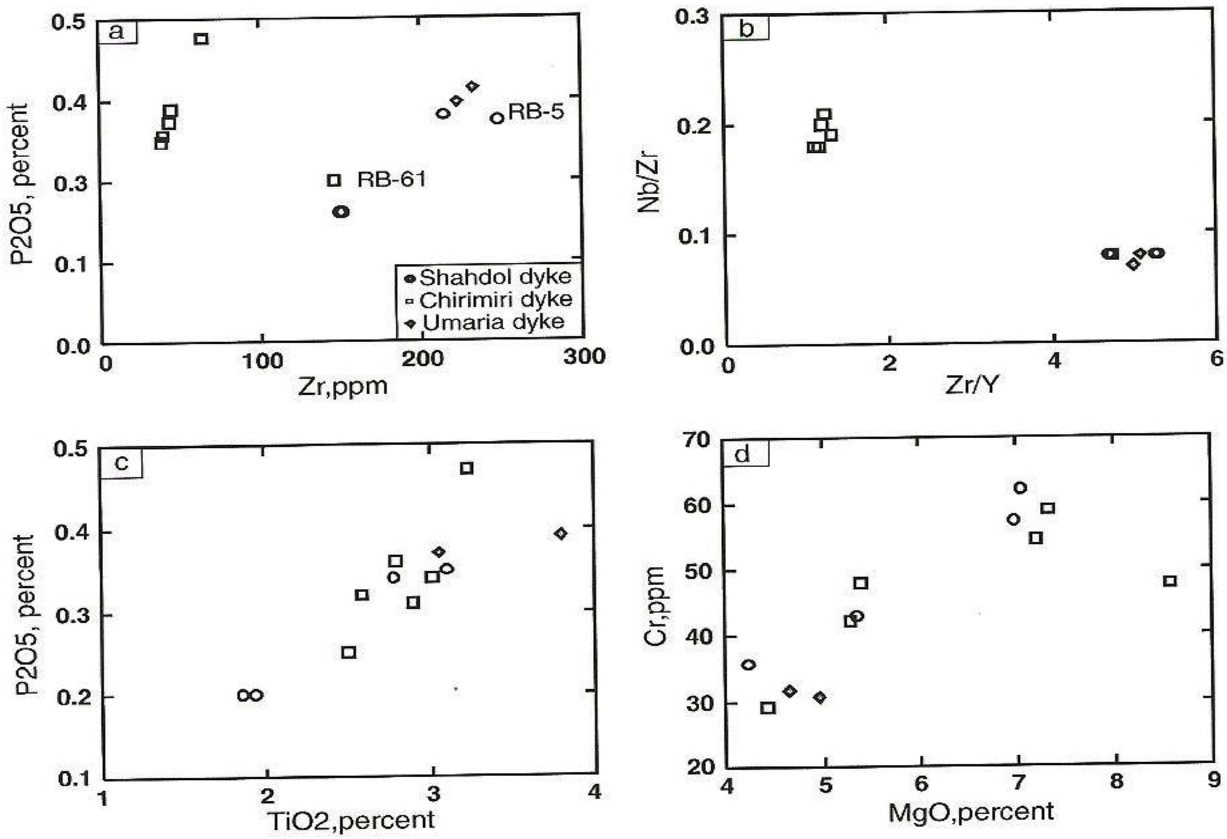

Fig. 9.5 Interelemental variation in Rewa dykes. (**a**) Variation of P_2O_5, percent vs Zr, ppm, showing two groups; Chirimiri dykes (*square*) and the Shahdol dykes, reflect contrasting Zr abundances. A positive correlation exists for the two groups separately. (**b**) Nb/Zr vs Zr/Y for all the dykes. (**c**) P_2O_5, percent vs TiO_2, percent, illustrating a strong positive correlation. (**d**) Plot of MgO, percent vs Cr, ppm showing positive correlation as a result of fractional crystallisation. Sample RB 75 is away from the main trend. All the symbols are as in Fig. 9.5a

10–40 times over the primitive mantle abundances. We have compared the primitive mantle-normalised average trace element abundances of the Rewa dykes with those of Sangamner (Bondre et al., 2006), Pachmari (Sheth et al., 2009) and Salma dyke (Kent et al.1997) in Fig. 9.8, taking data from Table 9.6. There is a striking similarity in the distribution patterns (Fig. 9.7).

Among all the samples ΣREE shows a significant positive correlation with SiO_2, TiO_2, K_2O, P_2O_5, Ba, Rb, Sr, Nb, Ga, V, Hf and Sc but negative correlation with MgO, Co. This would suggest fractionation of plagioclase and clinopyroxene (Sen, 1995) in the samples.

Sr-Nd Isotope Geochemistry

Analytical Methods

About 75–100 mg of representative rock powders were digested with triple distilled concentrated HNO_3 and HF in Teflon vials. About 50 mg of ^{87}Rb, ^{84}Sr and mixed

Table 9.5 Rare earth elements and Sr-Nd isotopic data of Rewa dykes

Sample I.D	RB64	RB60	RB304	RB-68a	RB-66	RB112	RB110	RB-75	RB61	RB-5	RB-13b	13d	JB2	JB-2 Certified value[a]
La	11.2	9.20	17.2	10.5	16.3	14.5	16.0	8.12	9.91	18.8	10.4	10.7	2.36	2.37
Ce	29.8	25.5	41.4	28.7	43.3	40.8	42.8	23.2	25.55	46.5	26.5	27.2	6.87	6.77
Pr	3.62	3.23	4.65	3.56	5.24	4.88	4.9	2.99	3.06	5.28	3.15	3.2	0.95	0.96
Nd	22.7	21.3	27.4	22.6	32.9	29.9	28.5	19.8	18.5	30.6	18.8	19.3	6.66	6.7
Sm	5.74	5.79	6.9	5.68	8.00	7.96	7.2	5.40	5.10	7.75	5.08	5.02	2.28	2.25
Eu	2.05	2.05	2.07	2.01	2.74	2.47	2.28	2.03	1.64	2.53	2.09	1.81	0.88	0.86
Gd	6.98	7.08	8.89	6.96	9.59	9.54	8.68	6.75	6.44	9.66	6.36	6.47	3.14	3.28
Tb	1.11	1.19	1.36	1.18	1.57	1.52	1.41	1.10	1.02	1.52	1.04	1.04	0.62	0.62
Dy	6.12	6.14	6.80	6.34	8.38	7.63	7.16	6.05	5.12	7.80	5.41	5.27	3.70	3.66
Ho	1.20	1.17	1.37	1.23	1.66	1.50	1.45	1.16	1.02	1.57	1.05	1.09	0.82	0.81
Er	3.74	3.50	4.10	3.80	5.08	4.46	4.54	3.52	3.11	4.64	3.17	3.27	2.67	2.63
Tm	0.60	0.57	0.64	0.62	0.83	0.67	0.72	0.55	0.48	0.72	0.49	0.51	0.44	0.45
Yb	3.11	2.68	3.42	3.10	4.20	3.65	3.92	2.77	2.58	3.78	2.53	2.61	2.48	2.51
Lu	0.46	0.39	0.51	0.45	0.61	0.53	0.59	0.40	0.37	0.56	0.37	0.38	0.38	0.39
REE	98.47	89.72	126.72	96.67	140.40	130.01	130.05	83.83	83.96	141.69	86.38	87.80	–	–
87Sr/86Sr (t)	–	–	–	0.706213	0.709416	0.705326	0.704625	0.707651	–	0.705679	0.709434	0.714403	–	–
143Nd/144Nd (t)	–	–	–	0.511957	0.512669	0.512802	0.512629	0.512674	–	0.511677	–	0.512675	–	–
εNd(t)	–	–	–		2.25	4.83	1.46	2.34	–		–	2.35	–	–

[a]JB-2: Govindraju K (1994).

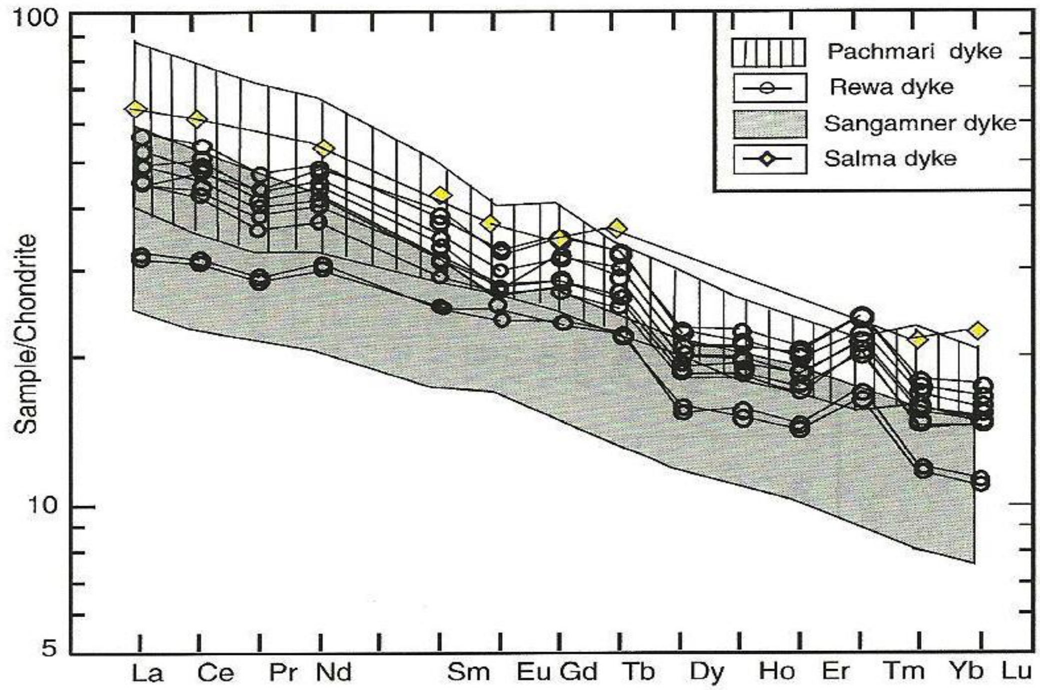

Fig. 9.6 Chondrite-normalised rare earth element abundances in mafic dykes (Rewa data from Table 9.3), Pachmari (Sheth et al., 2009), Sangamner (Bondre et al., 2006) and Salma (Kent et al., 1997) dykes. The chondritic abundance values are from Evensen et al. (1978)

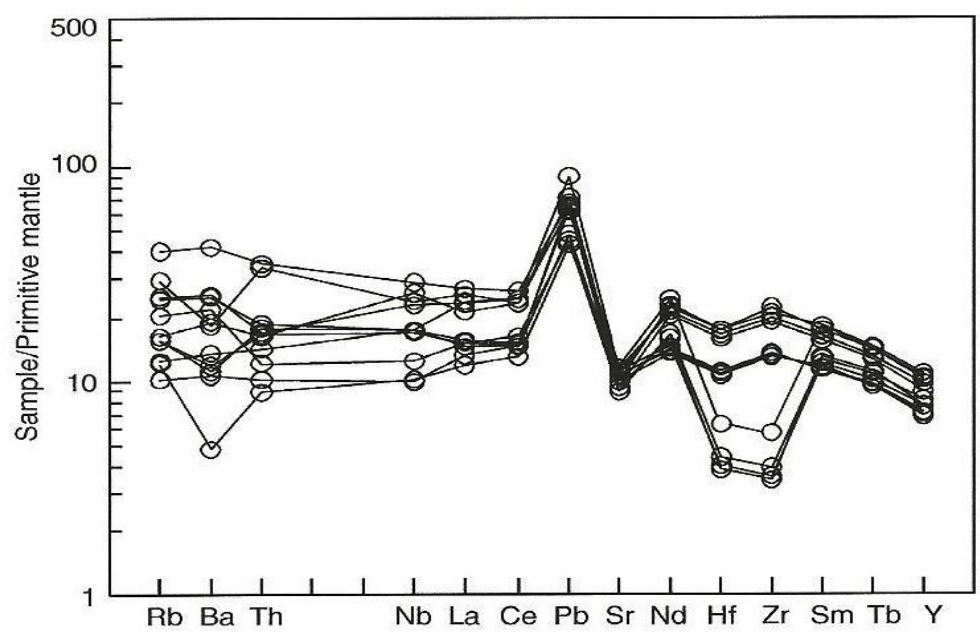

Fig. 9.7 Primitive mantle-normalised (Sun and McDonough, 1989) element patterns for Rewa dyke samples. Note the prominent Pb peaks and Zr-Hf troughs

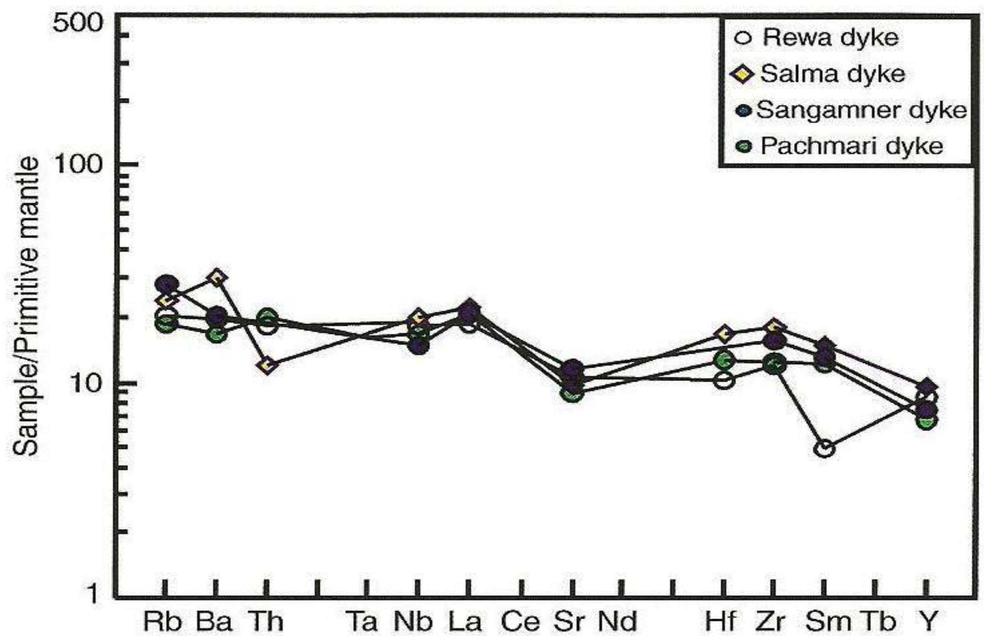

Fig. 9.8 Primitive mantle – normalised element (Sun and McDonough, 1989) patterns comparing the average abundance values of Sangamner, Pachmari and Salma dykes. The data is included in Table 9.6

^{150}Nd-^{149}Sm spikes with concentrations of 3.056, 8.4559, 0.78252 and 0.66519 μg/g respectively were added to the rock solutions.

Rb, Sr and REE were separated using HCl acid eluents with Bio-Rad AG 50W-X8 200–400 mesh H^+ form cation exchange resin. Sm and Nd were separated from the REE fraction by using LN Spec (Part No C-50) resin from Eichrom. Nd and Sm were eluted with 0.25 N HCl and 0.75 N HCl respectively. Isotopic analyses were carried out using a fully automatic Thermo Fisher TRITON multi-collector Thermal Ionisation mass spectrometer at the Indian Institute of Technology, Roorkee.

Rb, Sr, Sm and Nd concentrations in sample were calculated off-line after correcting for fractionation according to the double spike correction method. The isotopic compositions ^{87}Sr/^{86}Sr and ^{143}Nd/^{144}Nd were also re-calculated with the corrections for spike contribution. Reproducibility of the concentration measurements is monitored periodically by measuring the concentration of these elements in USGS rock standards. The total procedure blank in the laboratory at the present time is less than 8 ng of Sr and less than 1 ng for Nd.

The ^{87}Sr/^{86}Sr ratios were normalized to ^{86}Sr/^{88}Sr $= 0.1194$. Mean value for NIST Sr standard SRM-987 was ^{87}Sr/^{86}Sr $= 0.710248 \pm 20\ (2\sigma)$. The ^{143}Nd/^{144}Nd ratios were normalized to ^{146}Nd/^{144}Nd $= 0{\cdot}7219$. Average value for the Japanese Nd standard JNdi-1 was $0{\cdot}512108 \pm 16(2\sigma)$.

Table 9.6 Compositional variation of mafic dykes from Deccan Volcanic Province

		Rewa (present study)		Sangamner		Pachmari	
	Salma	Range	Avg (n = 12)	Range	Avg (n = 27)	Range	Avg (n = 18)
SiO_2	49.55	47.3–50.9	49.05	49.02–52.31	50.05	48.40–50.64	49.25
TiO_2	2.91	1.85–3.80	2.79	1.29–3.27	2.52	2.10–3.27	72.5
Al_2O_3	12.2	12.2–15.9	14.03	11.93–14.57	13.13	11.80–12.87	12.35
Fe_2O_3(t)	16.44	13.0–16.1	14.66	11.16–17.32	15.02	15.12–17.26	15.06
MnO	0.22	0.16–0.20	0.18	0.16–0.24	0.21	0.17–0.28	0.21
MgO	5.57	4.32–8.57	5.95	4.76–8.97	5.84	4.46–7.15	6.28
CaO	9.95	7.95–10.47	9.40	9.18–11.27	9.98	9.58–11.44	10.31
Na_2O	2.36	1.85–2.93	2.42	1.83–2.69	2.45	1.47–2.14	1.95
K_2O	0.57	0.36–0.82	0.56	0.20–0.99	0.41	0.16–0.78	0.46
P_2O_5	0.29	0.2–0.39	0.33	0.14–0.40	0.25	0.18–0.42	0.26
Trace elements, ppm							
Sc	43	28.9–39.8	34.8	26–38	31.7	31.89–38.96	34.81
V	414	314–498	401	246–489	338	354.3–512.8	419.13
Cr	84	29.1–58.8	45.1	41–557	144.7	237.30–684.3	480.53
Co	–	46.3–80.1	65.0	44–54	43.6	44.33–57.92	49
Ni	65	16.1–54.0	25.6	41–228	81.3	37.42–88.37	64.15
Rb	15	6.4–25.5	13.0	10–35	18.15	2.06–24.65	11.75
Sr	205	186–277	222	203–287	242.8	161.90–241.20	189.03
Sm	6.53	5.02–8.00	2.15	3.51–7.47	5.72	4.31–7.61	5.42
Y	43	30.8–47.0	38.8	17–46	34.2	25.49–38.69	30.24

Table 9.6 (continued)

	Salma	Rewa (present study)		Sangamner		Pachmari	
		Range	Avg (n = 12)	Range	Avg (n = 27)	Range	Avg (n = 18)
Zr	199	38.5–247.8	133	104–237	171.8	114.10–227.40	138.3
Nb	14.2	7.09–20.8	12.8	7–17	10.5	7.32–20.80	11.78
Ba	211	74.0–292	134	62–225	141.9	70.14–310.7	115.32
La	15.2	8.12–18.8	12.7	9.20–21.6	15.8	9.42–24.18	14.37
Ce	37.6	23.2–46.5	33.4	22.1–50.7	37.26	21.67–52.55	32.37
Yb	3.72	2.53–4.20	3.19	1.54–3.91	2.83	2.54–3.86	3.03
Lu	0.58	0.37–0.61	0.47	0.22–0.48	0.405	0.34–0.52	0.45
Hf	5.13	1.23–5.34	3.16	–	–	2.98–5.76	3.89
Ta	0.89	0.53–4.28	1.73	–	–	0.42–1.22	0.67
Th	2.02	0.76–3.01	1.55	–	–	3.19–1.29	1.68
Isotopic abundance							
$(^{87}Sr/^{86}Sr)i$	0.70482	0.704625–0.714403		0.70555–0.70877		0.70516–0.71589	
$(^{143}Nd/^{144}Nd)i$	0.512667	0.511677–0.512802		0.511923–0.512784		0.512594–0.512689	
εNdi	1.00	1.46–4.83		–13.4 to 3.00		0.8–110.9	

Reference: Salma: Kent et al. (1997); Sangamner: Bondre et al. (2006); Pachmari: Sheth et al. (2009).

Isotopic Results

The Nd-Sr isotopic compositions of seven dyke samples analyzed in the present study are given in Table 9.5. All isotopic ratios have been time-corrected for 65 Ma, the age of Deccan volcanic eruption.

The measured $^{87}Sr/^{86}Sr$ ratios of the dykes range from 0.704667 to 0.71447. The corresponding $(^{87}Sr/^{86}Sr)i$ values vary from 0.704625 to 0.714403. The Sr isotopes are distinctly more radiogenic, excepting sample RB 110 that has a low $(^{87}Sr/^{86}Sr)_i$ ratio of 0.704625, compared to normal mantle-derived rocks. Measured $^{143}Nd/^{144}Nd$ in all the seven samples vary from 0.511677 to 0.512871. For analytical uncertainty, the initial $^{143}Nd/^{144}Nd$ of two samples. RB 5 and RB 68 a, could not be calculated. The initial $^{143}Nd/^{144}Nd$ values of the remaining five samples, RB 66, RB 75, RB 13d, RB 110, and RB 112, vary from 0.512629 to 0.512802 (εNd = + 1.46–+ 4.83) (Table 9.5; Fig. 9.9). Considering the Sr and Nd isotopic

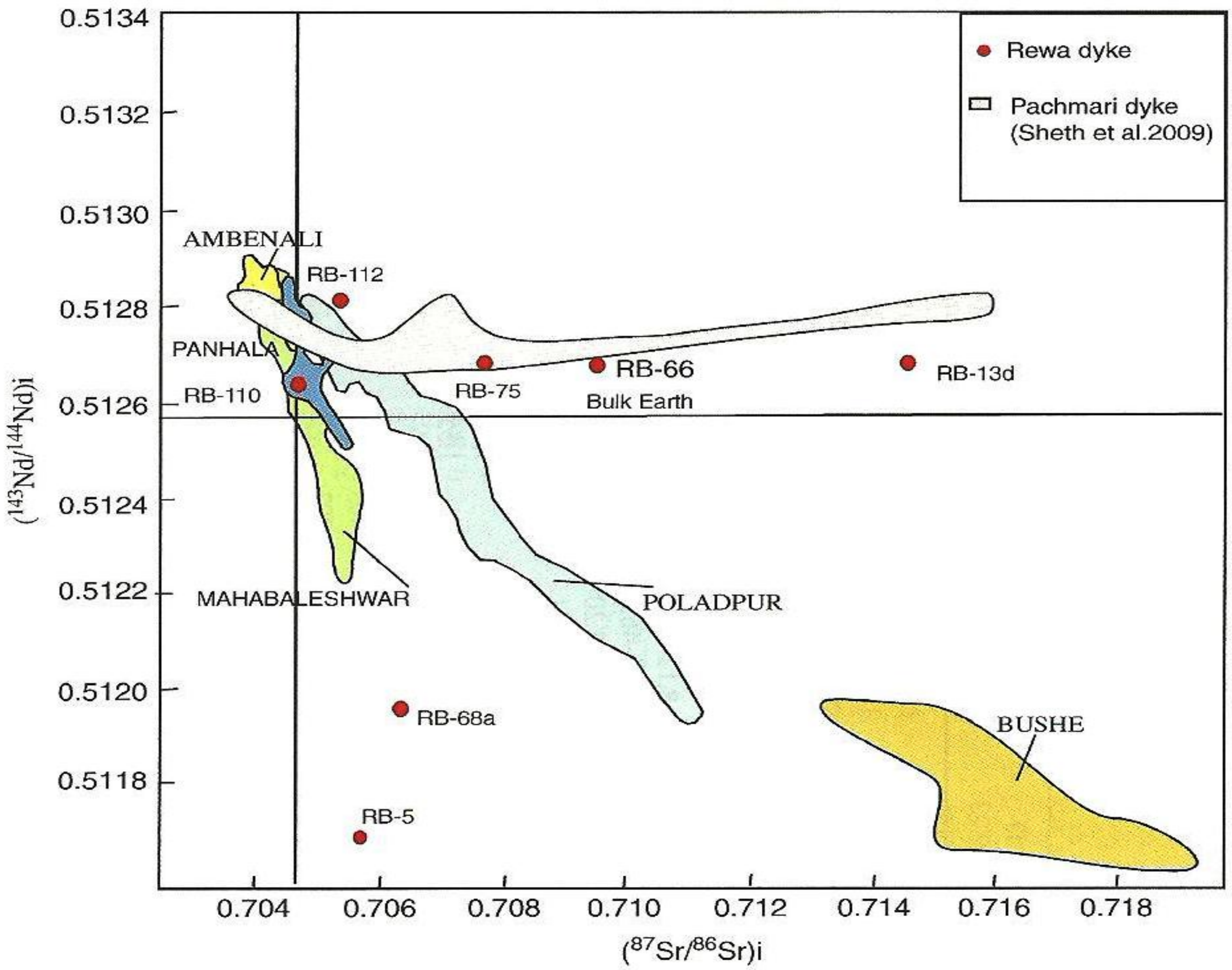

Fig. 9.9 Sr-Nd isotopic data for Rewa dykes (this study) compared with the standard south western Deccan Formations (Lightfoot and Hawkesworth, 1988). Also included is the field for Desur sub unit (after Cox and Hawkesworth, 1985). For sample numbers RB 5 and RB 68a, the measured $^{143}Nd/^{144}Nd$ are plotted. Sr and Nd isotopic compositions obtained on standards are indicated in the text. Also plotted are Sangamner (Bondre et al., 2006) and Pachmari (Sheth et al., 2009) dykes

composition, the samples can be grouped in two groups: one having a nearly constant Nd isotopic abundance but variable Sr isotopic composition, and the other having nearly constant $^{87}Sr/^{86}Sr$ at 0.706 but lower $^{143}Nd/^{144}Nd$ values (Fig. 9.9). Petrographical characters of the samples do not indicate pervasive alteration. Taken all the samples together, LOI (Table 9.2) has a positive correlation with Sr, Rb and Ba but has no relationship with the Sr and Nd isotopic composition. For example, RB 5 has highest Rb of 25.5 ppm, Ba (292 ppm) and Th (3.01 ppm) (Table 9.2) but the initial $^{87}Sr/^{86}Sr$ ratio, 0.705679, is among the lowest. In the case of dyke RB 13 d, the initial $^{87}Sr/^{86}Sr$ ratio of 0.7144403 and the concentations of the elements Rb, Ba and Th are low. We therefore conclude that the isotopic composition has not been affected by alteration.

There is no relation between $^{87}Sr/^{86}Sr$ ratios and SiO_2 or 1/Sr ratios ruling out simple crustal contamination. The Sr, Nd isotopic characters in the south western Deccan Formations have been generally interpreted as simple mixing between an Ambenali-type magma with a lithospheric mantle end member (Sheth et al., 2009). A more complicated two-stage mixing has been proposed for these Formations by Peng et al. (1994) to explain the Nd-Pb isotopic arrays. We explain the observed variable Sr, Nd isotopic composition of five Rewa dyke samples (RB 110, RB 112, RB 75, RB 66, RB 13d) by binary mixing between an Ambenali-type magma and a lithospheric end member with enriched $^{87}Sr/^{86}Sr$ ($\sim$0.716) but almost constant $^{143}Nd/^{144}Nd$ around 0.5127.

Discussion

Mafic dykes constitute an important component of Large Igneous Provinces. Many researchers have taken up geochemical as well as isotopic studies to understand the relationship between the dykes and the flows. In an effort to establish linkage with established Deccan stratigraphy of the Western Ghats, dykes of the Western and Central Deccan Volcanic Province (DVP) have received attention. Details of the distribution of mafic dykes and their chemical characters for the northeastern part of the DVP are not available (Vanderkluysen et al., 2004). Such studies on the dykes from other regions such as the eastern and northeastern DVP are essential to develop a regional database. The present study is one such attempt on the mafic dykes of the Rewa Basin in the eastern most part of DVP. We examined regional compositional change of these dykes and the dispersal of Deccan magma on a wider context.

Regional Composition

The Son River dykes are more primitive with higher MgO and lower TiO_2 contents than other samples. Sen and Cohen (1994) established the contemporaneity of the Chala-Delakhari sill of Pachmari region and Deccan volcanism of the Western Ghats based on two ^{40}Ar–^{39}Ar ages of 66.1 ± 0.3 and 65.1 ± 0.3 Ma. We have compared the composition of the Pachmari and Sangamner mafic dykes with the Rewa dykes of the present study (Table 9.6). In the total alkali – silica diagram (Fig. 9.4) these dykes plot in the basalt field as do the Rewa dykes. The primitive mantle-normalised values of some trace elements of these dykes are plotted in Fig. 9.8. The Salma dyke of the Gondwana coalfield of the Rajmahal Province is also shown in this figure for a comparison. The normalised patterns are strikingly similar, except slightly enriched Ba and depleted Th in the Salma dyke. This similarity would suggest similar petrogenetic processes for the dykes.

The chondrite-normalised rare earth element patterns of Rewa, Pachmari and Sangamner along with the Salma dykes (Fig. 9.6) are also very similar, $(La/Yb)_n$ ratios of all the dykes vary within 2.1 and 3.6. Total REE contents are, however, variable. There is overlap in the chondrite-normalised fields with the Sangamner dykes having higher total REE, and Pachmari dykes having lower total REE than the Rewa dykes. The Salma dyke REE pattern is also similar but with a higher REE contents than the Rewa and Pachmari dykes. The Salma dyke has REE contents similar to the enriched Sangamner dyke samples. Sen and Cohen (1994) concluded that the Bushe, Poladpur and Ambenali Formations of the Western Ghats are chemically distinct from the northeastern lavas, the latter having low Ba, Rb and K.

The Sr and Nd isotopic data of the present study (Table 9.5) generally fall within the Sr-Nd isotopic range for the Deccan basalts. The range of $^{87}Sr/^{86}Sr$ in the Rewa samples (0.704625–0.714403) is within the reported values for Bushe Formation where pronounced crustal contamination has been established (Keays and Lightfoot, 2009, and many references therein). The Rewa and Pachmari dykes (Sheth et al., 2009) show a similar pattern with a flat mixing curve in a $^{87}Sr/^{86}Sr$ – $^{143}Nd/^{144}Nd$ plot (Fig. 9.9). The mafic *basaltic flows* of the Rewa basin also display a broadly similar Sr-Nd isotopic relationship (our unpublished data). The εNd values of both Rewa and Pachmari dykes are positive. Barring two samples, RB 68a and RB 5, the Rewa dykes have εNd values from + 1.46 to + 4.83. Mixing between two end members, an Ambenali-type magma and another with high $^{87}Sr/^{86}Sr$ would be required to derive the Sr-Nd array of these samples (Fig. 9.9) (*cf.* Yan et al., 2008). But to obtain the isotopic composition of RB 68a and RB 5 (Fig. 9.9) mixing between an Ambenali-type end member with another component with low Sm/Nd or $^{143}Nd/^{144}Nd$ around 0.5117 is required.

Dispersal and Migration

It is well known that the Deccan volcanic rocks attain the highest thickness, 2 km, in the Western Ghats, and gradually thin down towards east. In Amarkantak (Fig. 9.2) the thickness of the Deccan flows is estimated at 170 m (Geological Survey of India, 1995). Towards east, in and around Shahdol, the thickness of Deccan volcanic rocks is about 30 m overlying the Gondwana sediments. The frequency and number of mafic dykes in the Deccan rocks are also high in the west than in the east. The dominant dyke occurrences have been shown in Fig. 9.2. Whether the mafic dykes are the feeder to the Deccan flows is a subject of intense discussion. Recently Sheth et al. (2009) have discussed the difficulty of dyke-sill-flow relation from geochemical characters for the Pachmari dykes. Occurrence of volcanic vents with emanating dykes and feeding the flows has also been discussed (Misra, 2001, 2008). In the eastern DVP, the relation between the flows and the dykes has not been established from field relations. It is not known if separate vents of volcanic eruption exist in this part. However from the gradual diminishing thickness of the lava sequences, it appears that the flows migrated eastward from the western part (West, 1959). The reported age of 64.4 Ma for the Salma dyke (Kent et al., 1997) near the 115 Ma Rajmahal Volcanic Province in eastern India suggests contemporaneity of the former with the Deccan volcanics. Besides the Salma dyke, there are other Tertiary dykes in the vicinity of Rajmahal. In our earlier discussion we have shown the similarity of the geochemical characters of Salma with the Rewa dykes. Kent et al. (1997) suggested that the Tertiary dykes of eastern India are chemically and isotopically similar to the ferro-basaltic lavas from the upper Deccan Formations of Western Ghats. It is known that in the Raniganj (Gondwana) basins of eastern India, there are ultramafic alkaline dykes of kimberlitic (Group II) affinity which are about 115 Ma old (Kent et al., 1998), very similar to the age of the Rajmahal volcanic rocks (Baksi et al.,

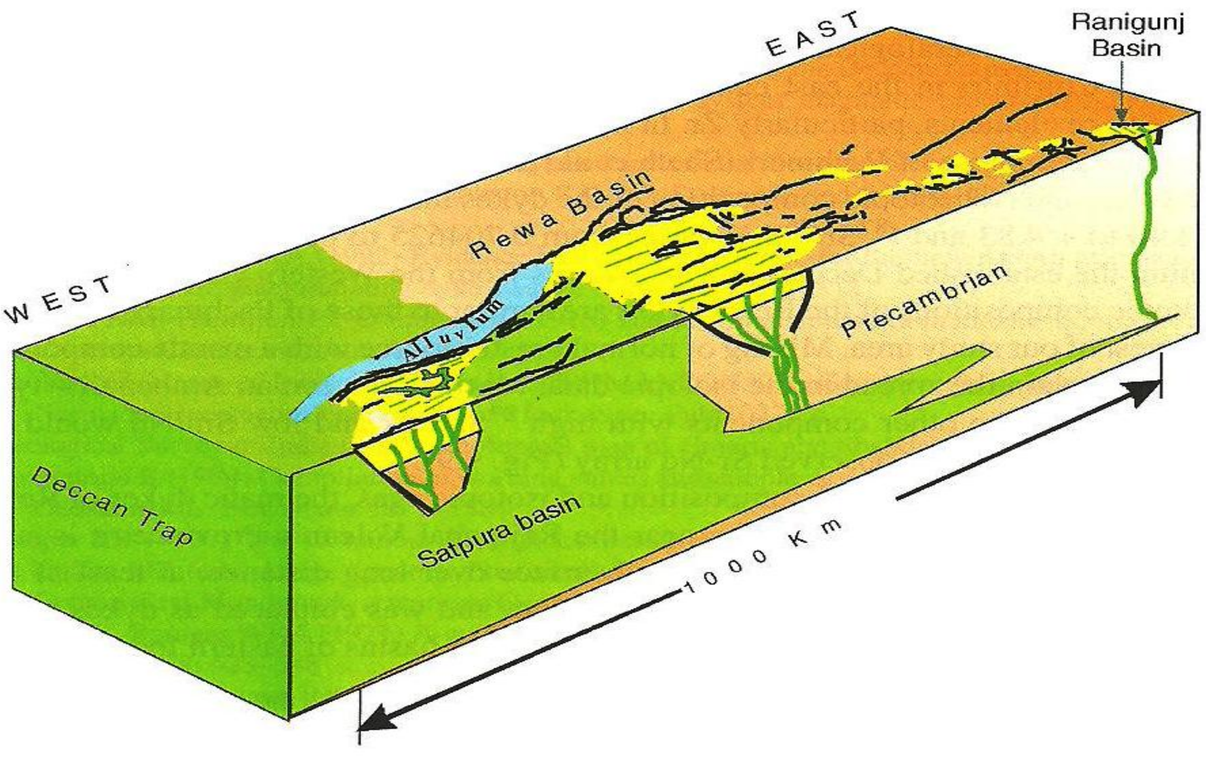

Fig. 9.10 Schematic diagram showing possible subsurface migration of Deccan magma from western India eastward and emplacement as dykes in the western periphery of DVP and the Gondwana basins of Rewa, Raniganj and other basins of eastern India along intrabasinal faults as pathways. Chemical similarity and $^{39}Ar-^{40}Ar$ age of 64 Ma for the Salma dykes seem to support the migration of magma

1987). Example of long distance migration of basaltic lava flow could be cited from the Pomona flow of the Columbia River basalt province that has been traced for almost 600 km from its source (Hooper, 1997), and the chemical and mineralogical homogeneity across long distances were interpreted to indicate *exceptionally* high flow rates.

Combining the field occurrences and the geochemical attributes it is suggested that Deccan magma migrated eastward subsurface from the western part (see also Paul, 2005) and was emplaced as dykes using the intrabasinal faults of the Gondwana basins as pathways (Fig. 9.10) over a distance of more than 500 km. The diminishing thickness of the Deccan volcanics as also the rare occurrence of mafic dykes in the eastern part could follow from the supply of magma. Migration of mafic magma over distances of 2,000 km for the Mackenzie dykes (Ernst and Baragar, 1992) or for a distance ranging from 150 to 350 km for the Pachmari dykes (Sheth et al.,2009) or north eastern Deccan lavas for over 900 km (Peng et al., 1998) also has been suggested.

Conclusions

The mafic dykes from the eastern part of Deccan Volcanic Province are of uniform chemical and mineralogical composition. Between the dykes two groups at Shahdol and the Chirimiri in the east can be identified on the basis of MgO content and some trace elements, particularly Zr. In major element composition the Rewa dykes are similar to those of Pachmari (Sheth et al., 2009) and Sangamner (Bondre et al., 2006). Sr and Nd isotopic composition of the dykes indicate a spread of (εNd)i from + 1.46 to + 4.83 and ($^{87}Sr/^{86}Sr$)i varies from 0.704625 to 0.714403. This range is within the established Deccan flow sequences from the Western Ghats. The Sr-Nd isotopic compositions of the Rewa dykes are similar to those of Pachmari, further to the west of our study area. Mixing of normal crustal source with a mantle component cannot explain the spread in the isotopic data. Mixing between an Ambenali – type magma with two other components with high $^{87}Sr/^{86}Sr$ and low Sm/Nd would be required to derive the observed Sr-Nd array (Fig. 9.9).

Comparing the chemical composition and isotopic ages, the mafic dykes of Rewa basin and the Tertiary dykes from near the Rajmahal Volcanic Province, it is suggested that Deccan magma travelled subsurface over long distance, at least of the order of 500 km, along the Narmada lineament and was emplaced as dykes along intrabasinal faults in Rewa and the other Gondwana basins of eastern India.

Acknowledgements We thank V Balaram and NN Murthy for help with the geochemical analyses and C Chakraborty for discussion on magma dispersal in the early stages. Comments of official reviewer, Ray W Kent, and the editor, Rajesh Srivastava, greatly improved the paper. We appreciate the comments of N C Ghose on an earlier draft. H N Bhattacharya extended various facilities at Presidency College, Kolkata. The Department of Science and Technology, Government of India provided financial support in the form a Research Fellowship to T Lala and a grant to D K Paul. DKP is grateful to the Indian National Science Academy for a Senior Scientist position during the course of this research.

References

Auden JB (1949) Dyke in western India – A discussion of their relationships with the Deccan Traps. Trans Nat Inst Sci India 3: 123–157

Baksi AK (1987) Critical evaluation of the age of the Deccan traps, India: Implications for flood basalt volcanism and faunal extinctions. Geology 15: 147–150

Baksi AK, Barman TR, Paul DK, Farrar E (1987) Widespread early cretaceous flood basalt volcanism in eastern India: Geochemical data from Rajmahal-Bengal-Sylhet Traps. Chem Geol 63: 133–141

Balaram V, Gnaneshwar R (2003) Rapid determination of REEs and other trace elements in geological samples by microwave digestion and ICP-MS. At Spectr 24(6): 206–212

Beane JE, Turner CA, Hooper PR, Subbarao KV, Walsh JN (1986) Stratigraphy, composition and form of the Deccan basalts, Western Ghats, India. Bull Volcanol 48: 61–83

Bhattacharji S, Chatterjee N, Wampler JM, Nayak PN, Deshmukh SS (1996) Indian intraplate and continental margins, rifting, lithospheric extension and mantle upwelling in Deccan Flow Basalt volcanism near the K/T boundary: Evidence from mafic dike swarms. J Geol 104: 379–398

Bondre NR, Hart WK, Sheth HC (2006) geology and geochemistry of the sangamner mafic dyke swarm, western Deccan volcanic orovince, India: Implications for regional stratigraphy. J Geol 114: 155–170

Chakraborty C, Mandal N, Ghosh SK (2003) Kinematics of the Gondwana basins of Peninsular India. Tectonophysics 377: 299–324

Chandrasekharam D, Mahoney JJ, Sheth HC, Duncan RA (1999) Elements and Nd-Sr-Pb isotope geochemistry of flows and dikes from the Tapi rift, Deccan flood basalt province. India J Volcanol Geothermal Res 93: 111–123

Cox KG, Hawkesworth CJ (1985) Geochemical stratigraphy of the Deccan Traps at Mahabaleswar, Western Ghats, India with implications for open system magmatic processes. J Petrol 26: 355–377

Deshmukh SS, Sehgal MN (1998) Mafic dyke swarms in the Deccan volcanic province of Madhya Pradesh and Maharashtra. In: Subbarao KV (ed) Deccan Flood basalts. Geol Soc India Mem 10: 323–340

Ernst RE, Baragar WRA (1992) Evidence from magnetic fabric for the flow pattern of magma in the Mackenzie giant radiating dyke swarm. Nature 356: 511–513

Evensen NM, Hamilton PJ, O'nions RK (1978) Rare earth abundances in chondritic meteorites. Geochim Cosmochim Acta 42: 1199–1212

Geological Survey of India (1995) Project CRUMANSONATA, Geoscientific studies of the Son-Narmada Lineament Zone, Geol Surv India Spec Publ10371 p

Geological Survey of India (2005) Geological map of Umaria and Shahdol

Govindraju K (1994) Compilation of working values and sample descriptions for 383 Geostandards Geostandards. Newsletter 18: 1–158

Hooper PR (1997) The Columbia River flood basalt province: Current status. In: Mahoney JJ, Coffin MF (eds) Large Igneous Provinces: Continental, Oceanic and Planetary volcanism. Geophysical Monograph, American Geophysical Union 100: 1–27

Irvine TN, Baragar WRA (1971) A guide to the chemical classification of the common rocks. Can J Earth Sci 8: 523–548

Karkare SG, Srivastava RK (1990) Regional dyke swarms related to the Deccan Trap Alkaline Province, India. In: Parker AJ, Rickwood PC, Tucker DH (eds) A.A. Balkema, Rotterdam: 335–347

Keays RR, Lightfoot PC (2009) Crustal sulphur is required to form magmatic Ni-Cu sulphide deposits: Evidence from chalcophile element signatures of Siberian and Deccan Trap basalts. Miner Deposita doi: 10.1007/S00126–009–0271–1

Kent RW, Kelley SP, Pringle MS (1998) Mineralogy and Ar/Ar geochronology of orangeites (Group II kimberlites) from the Damodar Valley, Eastern India. Mineral Mag 62: 313–323

Kent RW, Malcolm S, Pringle R, Dietmar M, Saunders AD, Ghose NC (2002) 40Ar/39Ar geochronology of the Rajmahal basalts, India, India, and their relationship to the Kerguelen plateau. J Petrol 43: 1141–1153

Kent RW, Saunders AD, Kempton PD, Ghose NC (1997) Rajmahal Basalts, Eastern India: Mantle sources and melt distribution at a volcanic rift margin. In: Mahoney JJ, Coffin MF (eds) Large Igneous Provinces: Continental, Oceanic and Planetary volcanism. Geophysical Monograph, American Geophysical Union 100: 145–182

Le Bas MJ, Le Maitre RW, Streckeisen AL, Zanettin P (1986) A chemical classification of volcanic rocks based on the total alkali-silica diagram. J Petrol 27: 745–750

Lightfoot P, Hawkesworth CJ (1988) Origin of Deccan Trap lavas: Evidence from combined trace element and Sr-, Nd- and Pb-isotope studies. Earth Planet Sci Lett 91: 89–104

Misra KS (2001) Lava channel/tube network in western Maharashtra: Study of their morphology, formation and transportation of Deccan lava. Geol Surv India Spec Publ 64: 209–221

Misra KS (2008) Dyke swarms and Dykes within the Deccan Volcanic Province, India. In: Srivastava RK, Sivaji Ch, Chalapathi Rao NV (eds) Indian Dykes: Geochemistry, Geophysics and Geochronology. Narosa Publishing House, New Delhi: 57–72

Patil SK, Arora BR (2008) Palaeomagnetic and Rock magnetic studies on the intrusives from Raniganj basin, Damodar valley: Linkage to the Rajmahal Volcanics. In: Srivastava RK, Sivaji Ch, Chalapathi Rao NV (eds) Indian Dykes: Geochemistry, Geophysics and Geochronology. Narosa Publishing House, New Delhi: 511–526

Paul DK (2005) Petrology and geochemistry of the Salma dike, Raniganj coalfield (lower Gondwana), eastern India: Linkage with Rajmahal or Deccan volcanic activity? J Asian Earth Sci 25: 903–913

Paul DK, Lala T, Chaudhary AK (2008) Petrology and geochemistry of mafic flows and dykes of eastern Deccan Volcanic province, India. 33rd International Geological Congress, Oslo, Norway

Peng ZX, Mahoney JJ, Hooper PR, Harris C, Beane JE (1994) A role for lower continental crust in flood basalt genesis? Isotopic and incompatible element study of the lower six formations of the western Deccan Traps. Geochim Cosmochim Acta 58: 267–288

Peng ZX, Mahoney JJ, Hooper PR, Macdougall JD, Krishnamurthy P (1998) Basalts of the north-eastern Deccan Traps, India: Isotopic and elemental geochemistry and relation to south western stratigraphy. J Geophys Res 103: 29843–29865

Ray R, Sheth HC, Mallik J (2007) Structure and emplacement of the Nandurbar-Dhule mafic dyke swarm, Deccan Traps and the tectonomagmatic evolution of flood basalts. Bull Volcanol 69(5): 537–551

Sen G (1995) A simple petrologic model for the generation of Deccan Trap magmas. Int Geol Rev 37: 825–850

Sen G, Cohen H (1994) Deccan intrusion, crustal extension, doming and size of the Deccan-Reunion plume head. In: Subbarao KV (ed) Volcanism. Wiley Eastern, New Delhi: 201–216

Shanker R (1991) Thermal and crustal structure of "SONATA". A zone of mid-continental rifting in Indian shield. J Geol Soc India 37: 211–220

Sheth HC, Mahoney JJ, Chandrasekharam D (2004) Geochemical stratigraphy of Deccan flood basalts of the Bijasan Ghat section Satpura Range. India J Asian Earth Sci 23: 127–139

Sheth HC, Ray JS, Ranjini R, Vanderkluysen L, Mahoney JJ, Kumar A, Shukla AD, Das P, Adhikary S, Jana B (2009) Geology and geochemistry of Pachmari dykes and sills, Satpura-Gondwana basin, Central India: Problems of dyke-sill-flow correlations in the Deccan traps. Contrib Mineral Petrol doi. 10.1007/S 004010–009–0387–4

Srivastava RK, Singh SB, Karkare SG, Chandra R (1996) Geochemistry of Deccan volcanics and dykes from the Nisarpur and Manpur sections, Madhya Pradesh. Gond Geol Mag 2: 135–144

Sun SS, McDonough WF (1989) Chemical and isotopic systematics of oceanic basalt: implications for mantle composition and processes. In: Saunders. A.D., Norry, M.J (eds) Magmatism in the ocean basins Geol Soc London, Special paper 42, Blackwell Scientific publisher, 313–345

Vandamme D, Coutillot V, Besse J, Montigny R (1991) Paleomagnetism and age determination of the Deccan Trap (India): Results of a Nagpur-Bombay traverse and review of earlier work. Rev Geophy 29: 159–190

Vanderkluysen L, Mahoney JJ, Hooper PR(2004) Implications for the emplacement of the Deccan Traps (India) from isotopic and elemental signatures of dikes. EOS: Trans A Geophys Union 85(47) Fall Meet Suppl Abstarct V51B–0561

West WD (1959) The source of the Deccan trap flows. J Geol Soc India 1: 44–51

White RS, McKenzie DP (1989) Magmatism at rift zones: The generation of volcanic continental margins and flood basalts. J Geophys Res 94: 7685–7729

Yan J, Chen YF, Xu XS (2008) Geochemistry of Cretaceous mafic rocks from the Lower Yangtze region, eastern China: Characteristics and evolution of the lithospheric mantle. J Asian Earth Sci 33(3–4): 177–193